Modeling-Based Scale-Up of Reactors in Microwave-Assisted Chemistry

A Major Qualifying Project

Submitted to Faculty

of the

WORCESTER POLYTECHNIC INSTITUTE

in partial fulfillment of the requirements for the

Degree of Bachelor of Science

by

Andrew O Holmes

April 25, 2013

Approved:

Professor Vadim V. Yakovlev, Advisor

i

Abstract

Upgrading efficient reactions of microwave-assisted chemistry to the level of industrial technology is slowed down by physics-conditioned difficulties in development of large-scale and highly-productive reactors. This project addresses this issue by demonstrating that microwave reactors enhancing and accelerating chemical reactions can be designed with the help of computer optimization maximizing their energy coupling. We outline a computer-aided design approach based on the application of an efficient neural network optimization technique to a microwave reactor. This technique is used here to determine the geometry of a system considered as a direct enlargement of a small laboratory-scale reactor. Functionality and practicality of the technique is demonstrated by its application to the scale up of *MiniFlow 200SS* batch reactor from SAIREM SAS. Viability of the presented approach is illustrated by examples of three-parameter optimization of larger systems guaranteeing, for a given reactant, at least 90% energy efficiency.

Acknowledgement

I would like to thank:

- Office of the WPI Dean of Arts and Sciences and the Dean Karen Oates – for support of my 2012 summer research internship preceding this project;

- SAIREM SAS, Neyron, France – for providing the *MiniFlow 200SS* system – for experimentation and modeling;

- Dr. Marilena Radoiu, SAIREM SAS, R&D Director – for instructions and discussions of the design of *MiniFlow 200SS*;

- Prof. James Dittami, Department of Chemistry, WPI – for hosting *MiniFlow 200SS* system in his lab in the Gateway Park;

- Dr. Ethan K. Murphy, Applied Mathematics, Inc., Gales Ferry, CT – for his help with computational aspects of neural network optimization;

- Chuqiao (Vicky) Yang ('13) – for her partnership in experimentation with *MiniFlow 200SS* and cooperation in the development of its model.

Table of Contents

List of Figures and Tables

1. Introduction

Microwave-assisted chemistry (MAC) is a promising and rapidly growing interdisciplinary field utilizing microwaves as the means of enhancing and accelerating reactions in organic/inorganic chemistry, biochemistry, and other related disciplines. Microwave (MW) heating is the phenomenon behind such advantages of MAC as higher reaction rate, higher chemical yield, lower energy use, and some other benefits observed in comparison with conventional heating methods [1-3]. With special dedicated equipment for MAC now available, particular attention is currently paid to the development of well-controlled and reproducible reactions in large-scale production of chemical substances [3-6].

In order for MW-assisted reactions to become a widely accepted industrial technology, there is a need to develop equipment routinely producing new chemicals on a scale of kilograms. For instance, for pharmaceutical developments, $0.5 \div 5$ kg is the typically desired compound for initial clinical trials [4]. Moreover, some recent reports suggest that MW heating may become more energy efficient with the increase of the scale of the reaction [7]. There are known examples of demonstrated linear scale-up of MW chemistry from small tubes to slightly larger ones, cylindrical vessels, etc. [8-11]. However, upgrading successful processes of MAC to the levels of high productivity (and eventually to industrial

1

technologies) is still considered a challenging problem due to significant difficulties in development of large-scale reactors.

Currently, this problem is typically addressed via trial-and-error experiments aiming to find correlation between the input parameters of the scaled up MW reactors and the output chemical characteristics of the products [12, 13]. The efficiency of such studies is usually not high, their output is unpredictable, and the effort could be expensive. A fundamental reason for that is that ***microwave processing is not scalable*** – indeed, frequency in larger systems is the same whereas other characteristics change highly non-linearly. For instance, when the sizes of a MW system increase, distribution of the electric field becomes characterized by multiple extreme points, level of reflections of microwaves either increases or decreases, dissipated MW power decreases or increases, penetration of the electric field into a larger reactant usually decays (but there may be a focusing effect), etc. The fact that there is no possibility to monitor electromagnetic (EM) as well as thermal characteristics and conduct systematic observations of the ongoing reaction make the situation even more complicated.

Macroscopic modeling of the interaction of the reactants with the EM field in closed systems appears to be a powerful tool that can be used in the analysis of MAC reactors. Modeling may be useful in determining reflections from the MW system [12] as well as spatial distributions of dissipated power within the reactant [13]. There exist modeling techniques that can compute the temperature fields in the reactant by taking into account thermal and material parameters [13] and optimize MW reactors for energy efficiency [12].

In this context, the first goal of this project is

- **to develop and optimize a CAD model of an existing commercially available MW reactor.**
  The second goal is

- to demonstrate capabilities of modeling-based optimization and **find a scaled up system design that would be operational with a greater load volume in industrial MAC processes.**

The technique for direct CAD of MAC reactors was proposed for the first time in [12]. It suggests an approach based on the application of a neural network optimization technique to a MW system in order

to improve its coupling (and thus energy efficiency). Here we apply this approach to show how one could scale up the batch reactor *MiniFlow 200SS* designed, manufactured, and put on the market by SAIREM SAS (Neyron, France). While the operational volume of a liquid reactant in this reactor is about 10-15 ml, we determine configurations of enlarged reactors for the volume of the reactants of 200 ml. Energy efficiency of all obtained geometries is guaranteed to be at least 90%.

Therefore, overall, this MQP was designed to demonstrate that the laborious and expensive process of scaling up a particular MAC reactor can be made easier by using suitable techniques of modeling and optimization.

2. Microwave System and Its Model

2.1 Batch Reactor *MiniFlow 200SS*

Figure 2.1 shows the *MiniFlow 200SS* system which this MQP is focused on. This equipment was chosen for this project due to its innovative nature: the MW reactors are fed in *MiniFlow 200SS* by a solid-state generator that allows for robust control over the output MW power (from 0 to 200 W with the step of 1 W) and frequency (from 2.43 to 2.46 GHz with the step of 0.1 MHz).

While *MiniFlow 200SS* has a continuous flow reactor and a batch reactor, in this study we work with the latter. The reactor shown in details in Figure 2.2 consists of a cylindrical cavity containing a concentrically positioned cylindrical Teflon cup (visible in Figure 2.2 (b)) intended for holding the reactant in a cylindrical Pyrex vial. The resonator is fed via a coaxial cable (whose internal conductor is connected with a metal T-shaped structure inside the cavity). The reactant in the vial is put into the system through a cylindrical hole in the cavity's upper lid. Due to a large thickness of the lid, this hole serves as a cutoff waveguide preventing leakage from the cavity.

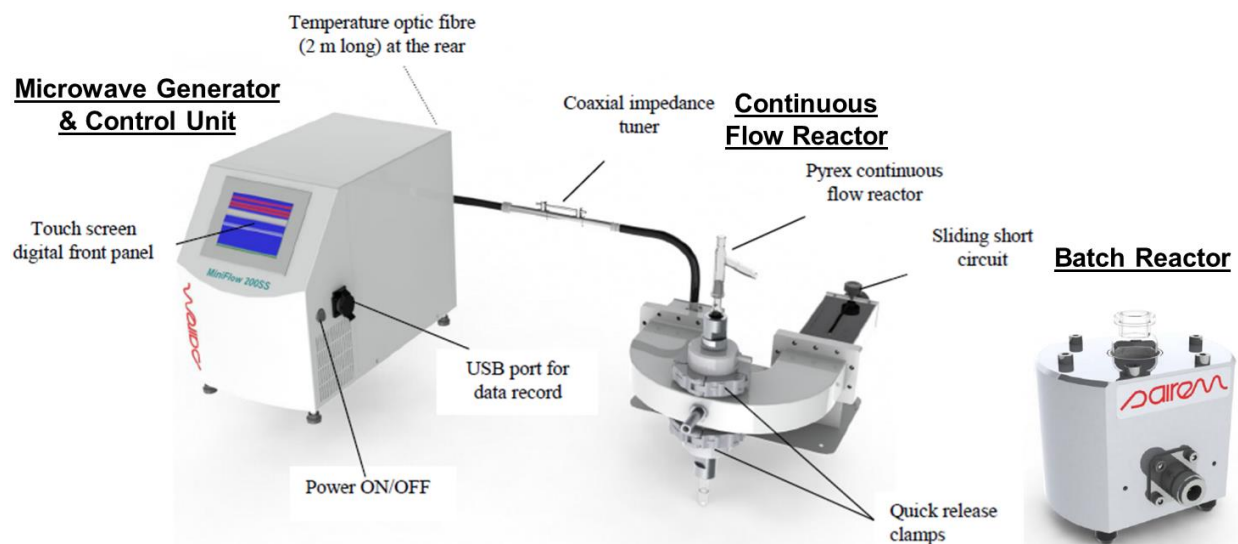Figure 2.1. SAIREM's *MiniFlow 200SS* system with the continuous flow and batch reactors.

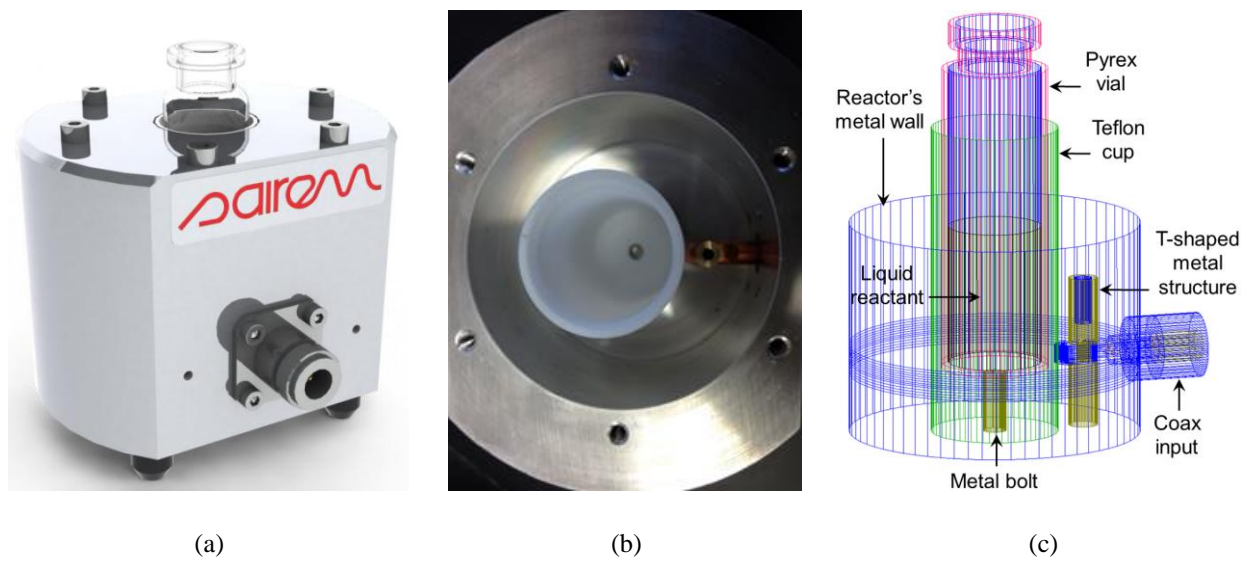(a)   (b)   (c)

Figure 2.2. *MiniFlow 200SS* batch reactor: general view (a), view of the interior with the upper lid removed (b), and

3D view of the interior of its reactor.

2.2 *QuickWave-3D* Model of *MinFlow 200SS*

The shape of the reactor has been reproduced in a 3D parameterized model developed for the full-wave 3D conformal FDTD simulator *QuickWave-3D* v. 2012 [14]. The development of the model was performed in two phases:

(a) reproduction of the 3D geometry of the system, and

(a) construction of optimal 3D FDTD mesh.

At the phase (a), all elements of the reactor have been constructed through a series of Boolean operations between multiple rectangular prisms and polygonal cylinders. To ensure that the geometry is reproduced adequately, the so-called Special Planes, i.e., the boundaries between the layers of the FDTD layers of cells, were placed on the necessary positions.

At the phase (b), the entire domain was discretized by a non-uniform mesh of rectangular cells constructed in accordance with the following conditions.

1) the geometry of the reactor's elements,

2) the wavelengths in the media,

3) the Courant Stability Condition, and

4) a conformal FDTD condition for the mesh near the media interface.

The Courant Stability Condition sets a restriction on the size of the time step; it should be proportional to the spatial step, i.e.:

$$\Delta t \le \frac{\Delta x}{v\sqrt{3}},$$

where v is speed of the EM field propagation in the medium (c in vacuum), we also follow the FDTD Rule of Thumb define by

$$\Delta x \le (0.05 \div 0.1)\lambda_m,$$

6
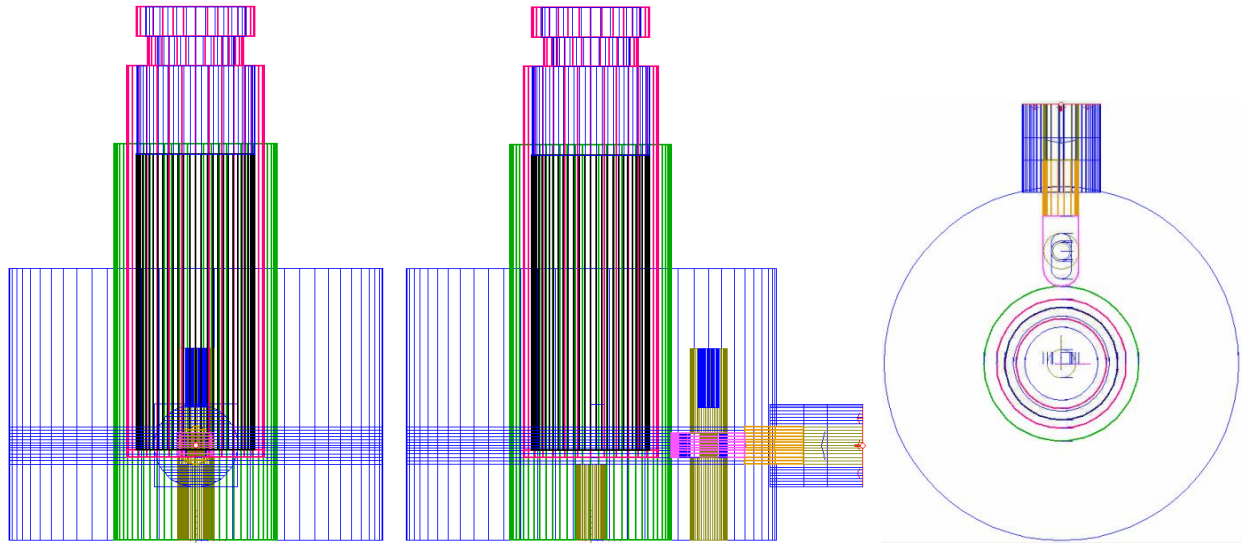
Figure 2.3. 2D views of the model in the coordinate planes.

where λ_m is the wavelength in the medium defined by

$$\lambda_m = \frac{c}{f\sqrt{\varepsilon}}$$

where f is free-space frequency and ε is relative dielectric constant. Condition 4) requires that there are no more than two different media in a cell.

After considering all these conditions, the domain is discretized with the minimum cell size of 0.2 mm, the entire FDTD mesh consists of 1.7 mil cells and the model requires about 160 MB of RAM.

The views of the resulting model in all three coordinate planes are shown in Figure 2.3. To ensure high accuracy of the solution of the EM problem, the scenario was discretized with a non-uniform mesh (with max cell sizes of 1.2 mm in air and 0.4 mm in the reactant) making 1.4 to 1.7 million cells depending on the height of reactant. In Figure 2.4, several positions of the Special Planes are illustrated on the views of the model in all three coordinate planes.

It has been detected that the simulations reach steady state after 30,000 time steps, so a single EM computation takes 25 to 30 min on Workstation A (see below Table 3.1).
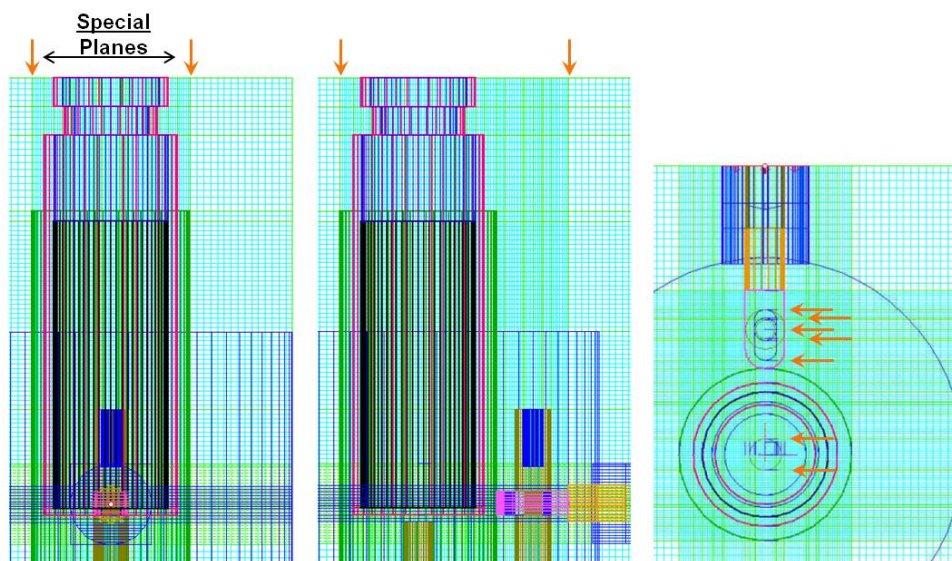
Figure 2.4. Typical Special Planes (marked by orange arrows) in the coordinate planes.

2.3 Verification of the Model

Due to the possibility of a rigorous control over frequency and power in the *MiniFlow 200SS* system, it was feasible to directly verify performance of the model against corresponding experiments.

In the absence of the equipment suitable for direct measurement of some EM characteristics (e.g., of reflections from the rector), it was a decision made to measure MW-induced temperature and computed temperature by coupling the EM solver with a thermal one.

Our experimental setup involving *MiniFlow 200SS* is shown in Figure 2.5. In our measurement, temperature of water was monitored using a fiber optic sensor (outer diameter 1.1 mm) which was held (except its tip) inside a glass capillary (internal diameter 1.5 mm) and was able to move along the central axis of the vial to measure temperature *in situ* at particular points inside the reactant.

On the modeling side, the EM simulator *QW-3D* was coupled with the FDTD-based thermal simulator, *Basic Heating Module* (*QW-BHM*) (a separate module in the *QW-3D* package). This combination allows one to simulate spatial evolution of 3D MW-induced temperature field. Experimental
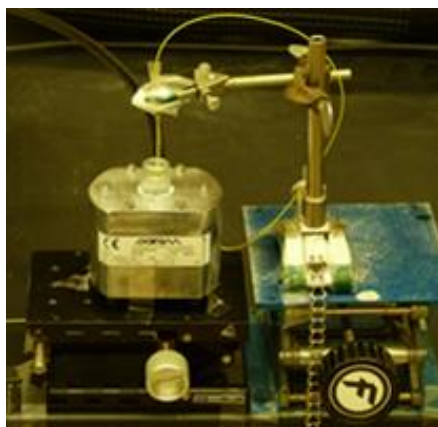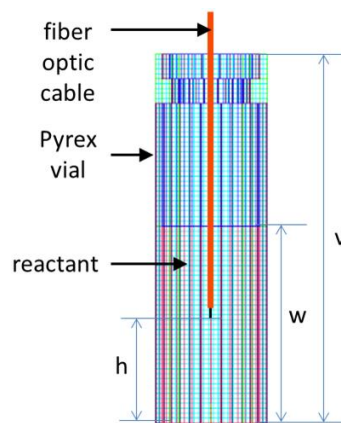
(a)   (b)

Figure 2.5. Experimental setup: *MiniFlow 200SS* with a fiber optic sensor inside a glass capillary vertically inserted

into the Pyrex vial (a) and a zoom-in view of the vial (b).

(a)   (b)

- ■ ● Experiment
- ——— Interpolated experimental data
- ——— Modeling
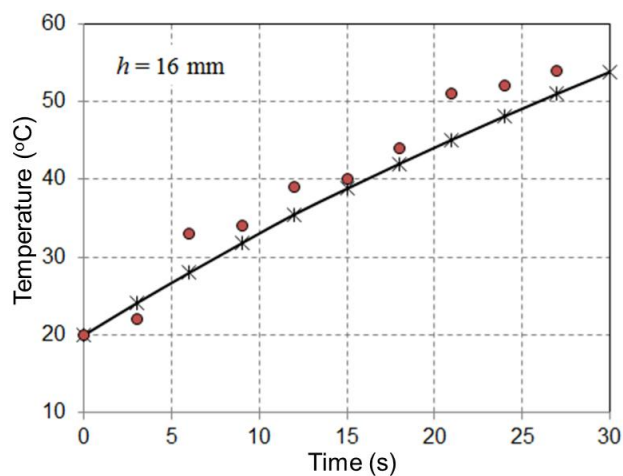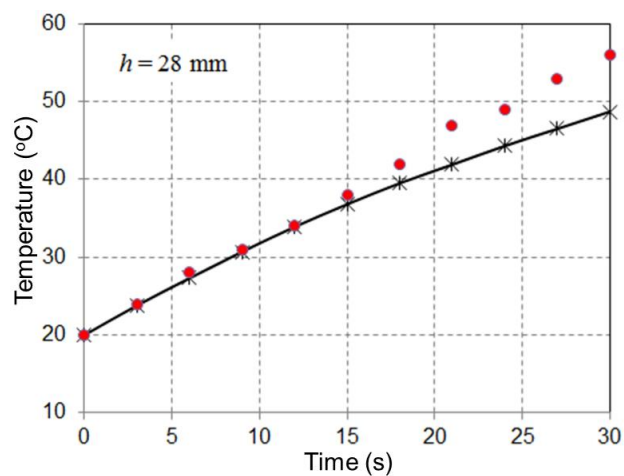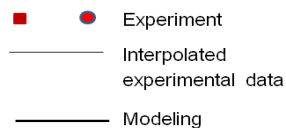
Figure 2.6. Temperature evolution at the heights 16 mm (a) and 28 mm from the bottom of vial for 15.6 g

of water heated by 100 W of microwave power – simulation and measurement.

9

data on EM and thermal material parameters of water were used in simulation. Temperature-dependent dielectric constant ε' and the loss factor ε'' at 2.45 GHz in the interval from 20°C to 90°C were taken from [15] whereas temperature-dependent density ρ, specific heat c, and thermal conductivity k were borrowed from [16].

It is seen from the graphs in Figure 2.6 that the experimental and modeling results are quite close: at the initial stage of heating, the divergence is less than 10%. This demonstrates an adequacy of the developed electromagnetic model.

3. Optimization Problem

3.1 Design of an Enlarged Reactor

In this project, we demonstrate functionality and practicality of the CAD technique suitable for scaling up MW reactors. The central point of the presented approach is: we consider an (existing and operational) *small lab-scale reactor* and **determine geometry of its enlarged analog** by numerical optimization. To ensure energy efficiency of the larger system, we employ a numerical model of the smaller reactor and use this model to generate **massive amounts of data for numerical optimization** determining an exact shape of the enlarged reactor.

More specifically, we intend to synthesize the dimensions of a MW system similar to *MiniFlow 200SS*, but larger in dimensions and suitable for handling larger loads. While a typical amount of a liquid reactant in a Pyrex vial (Figure 3.1 (a)) placed in *MiniFlow 200SS* is 10-15 ml, in the enlarged system, we set the goal to process 200 ml. To accommodate a significantly larger volume of the reactant in a scaled up analog of *MiniFlow 200SS*, we introduce a minor change in the original design. Since the diameter of the vial going through the hole in the lid cannot be increased, we consider a modified shape of the vial:

11

(a)   (b)
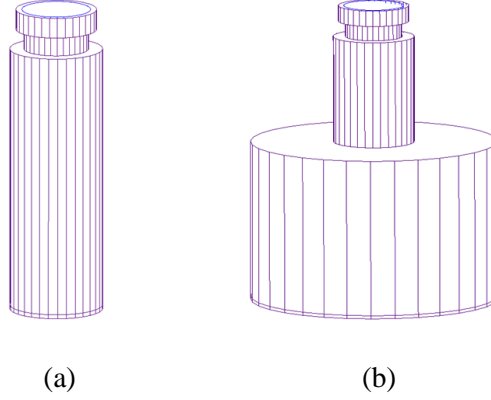
Figure 3.1. Pyrex vial of the *MiniFlow 200SS* batch reactor (a) and modified vessel for the

enlarged/optimized system.

instead of a straight cylinder, we now work with a vessel consisting of two cylindrical portions, as shown

in Figure 3.1 (b). Corresponding two-cylinder shape is also accepted for the Teflon cup surrounding the

vessel. The T-shaped structure used for excitation of the batch reactor is supposed to be of the same size,

but the Teflon cup is no longer required to be in direct contact with the tip of the excitation structure.

These changes in the design have been implemented in the *QW-3D* model of the enlarged reactor.

Some details of this modified model are given below (Section 3.2) while corresponding UDO scripts are

included in the Appendix. In this project, we employ this modified model to generate massive data for

subsequent numerical optimization.

3.2 Formulation of the Optimization Problem

Preliminary computational tests performed with the modified model and exemplified in Figure 3.3 show

that energy efficiency E (%) of the enlarged reactor operating at 2.45 GHz is quite different, but in all

cases is quite low; indeed, in a one-port MW system (which the considered reactor belongs to):

$$E(\%) = [1-(|S_{11}|)^2]100\%,$$

where $|S_{11}|$ is the magnitude of the reflection coefficient.
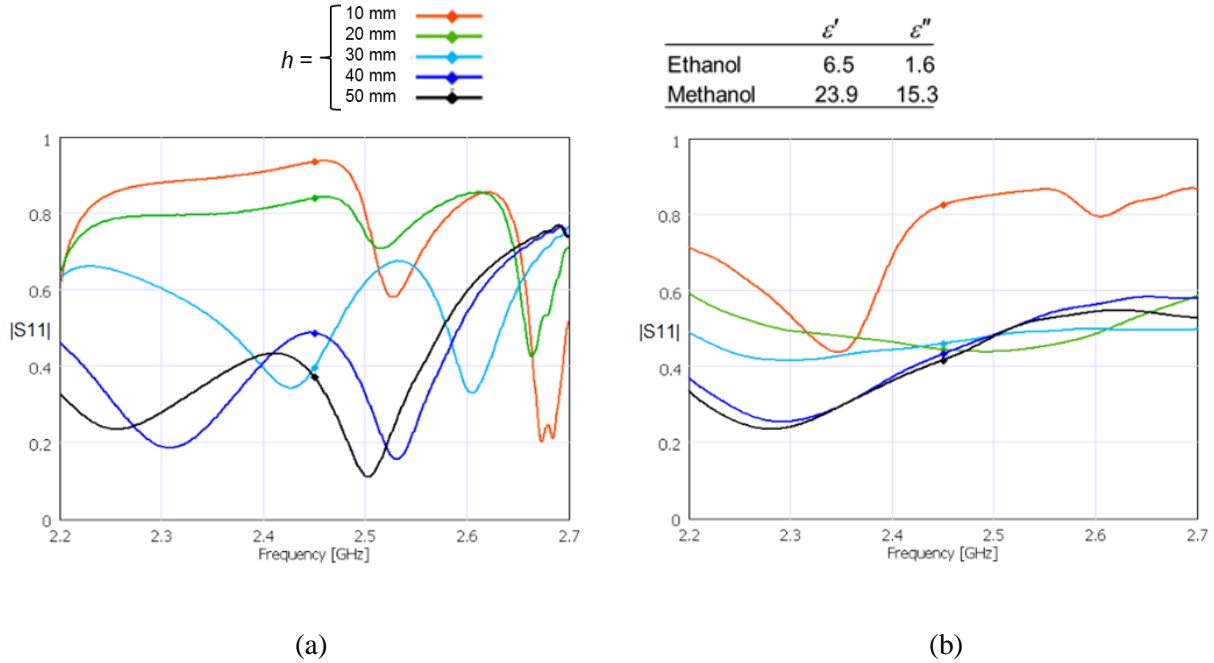
Figure 3.3: Typical non-optimized frequency charactistics of the reflection coefficient in the *MiniFlow 200SS* batch reactor with Ethanol (a) and Methanol (b) as the reactant.

As a result of a series of tests conducted as a sensitivity analysis of the system, we identified three geometrical parameters whose variations make an impact on the frequency characteristic of the reactor's reflection coefficient $|S_{11}|(f)$: thickness of the bottom of the Teflon cup (B) (Figure 3.4 (a)), outer diameter of the low cylinder of the vessel (T) (Figure 3.4 (b)), and inner diameter of the reactor's cavity (C) (Figure 3.4 (c)). These three parameters were chosen as design variables for optimization with the goal to find their values that guarantee much lower value of $|S_{11}|$ at 2.45 GHz.

More specifically, following the approach originally proposed in [16] and further developed in [12, 18, 19], we formulate the following optimization problem:

For a given reactant, find the values of B, T, C which yield less than E_r (%) of reflected microwave energy (i.e., $|S_{11}| < 0.1\sqrt{E_r}$) in W (%) of the frequency range (f_1, f_2). (*)
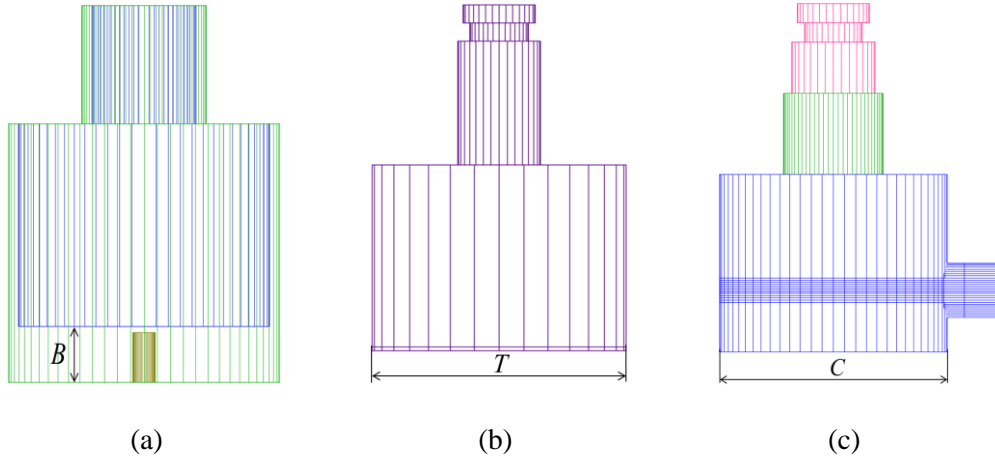
Figure 3.4. Elements of the enlarged reactor and design variables in optimization: Teflon cup and *B* (a), vessel
and *T* (b), reactor's cavity and *C* (c).

3.3 Optimization Technique

To solve Problem (*), we use an optimization technique based on the radial basis function (RBF) network
optimization algorithm originally introduced in [18] and principally upgraded in [19], featuring

i.   an objective function measuring the bandwidth of the frequency characteristic of the
      reflection coefficient over a specified frequency range, and

ii.   the constrained optimization response surface (CORS) technique [20] selecting additional
      sample points in the dynamic training of the network.

A brief general description of this optimization technique and its implementation is given in Figure 3.5.
The critical part of the algorithm is the choice of additional points: CORS sampling balances the goal of
finding the minimum with exploring unknown regions of the domain. This algorithm, backed by 3D
FDTD data is characterized by very quick convergence to the optima and a dramatic reduction in the
required number of underlying analyses. Due to these features, it is strongly favorable for viable
optimization of complex MW systems and/or structures with a large number of design variables.

	(a)	(b)
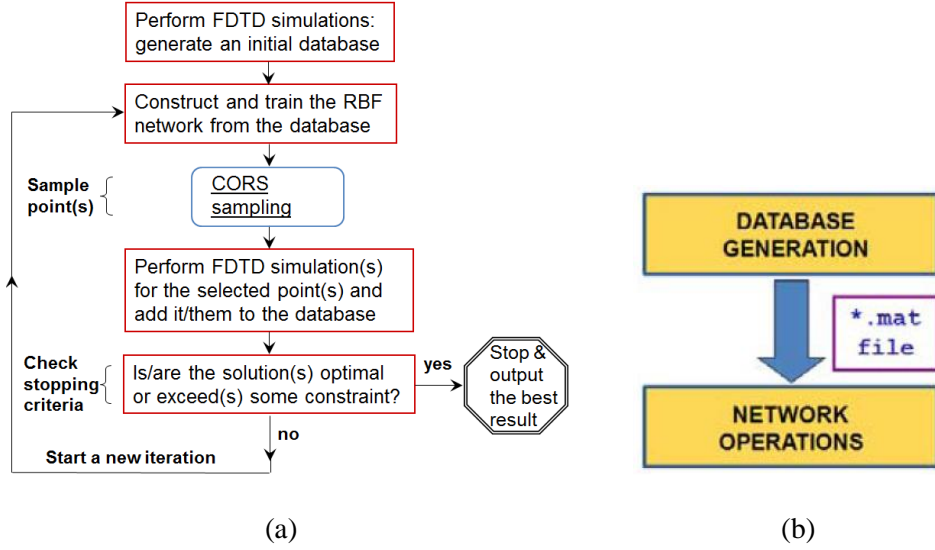
Figure 3.5. Flow chart of the RBF network optimization algorithm with CORS sampling (a) and modules of the

algorithm's MATLAB implementation (b) [12].

3.4 Input Data & Constraints

To demonstrate the use and operation of this optimization technique in application to the problem of scale-up of MAC system, we perform optimization for 200 ml reactant and apply the constraints:

<u>Constraints</u>: $W = 90\%$, $E_r = 9\%$, $(f_1, f_2) = (2.43, 2.47)$ GHz

<u>Design Variables</u>: $50 \leq T \leq 74$ mm, $90 \leq C \leq 134$ mm, and $0 \leq B \leq 10$ mm.

Due to the fact that the design variables T and C are mutually dependent, the problem is separated into three:

<u>Problem A</u>: $46 \leq T \leq 58$ mm; $98 \leq C \leq 110$ mm; $0 \leq B \leq 10$ mm

<u>Problem B</u>: $46 \leq T \leq 62$ mm; $102 \leq C \leq 118$ mm; $0 \leq B \leq 10$ mm

<u>Problem C</u>: $46 \leq T \leq 66$ mm; $106 \leq C \leq 126$ mm; $0 \leq B \leq 10$ mm

15

Figure 3.6. Optimization output: best frequency characteristics of the reflection coefficient for water – solution of

Problems A, B and C.

3.5 Optimization Results

The characteristics of $|S_{11}|(f)$ resulting from the performed optimization are shown in Figure 3.6; corresponding geometrical parameters of the optimized enlarged reactor are:

Water: Solution A: $T = 55.8$ mm; $C = 98.0$ mm; $B = 0$ with $W = 62.5\%$ $\rightarrow$ DB: 100 pts

Solution B: $T = 62$ mm; $C = 104.8$ mm; $B = 2.0$ mm with $W = 90\%$ $\rightarrow$ DB: 57 pts

Solution C: $T = 50$ mm; $C = 126$ mm; $B = 10.0$ mm with $W = 95\%$ $\rightarrow$ DB: 100 pts

where DB denotes the number of underlying FDTD analysis in generation of data points for the RBF neural network.

We also solve Problem B for 200 ml volumes of Ethanol and Methanol; the output of the performed optimization is shown in Figure 3.7; the resulting curves correspond to the following configurations:
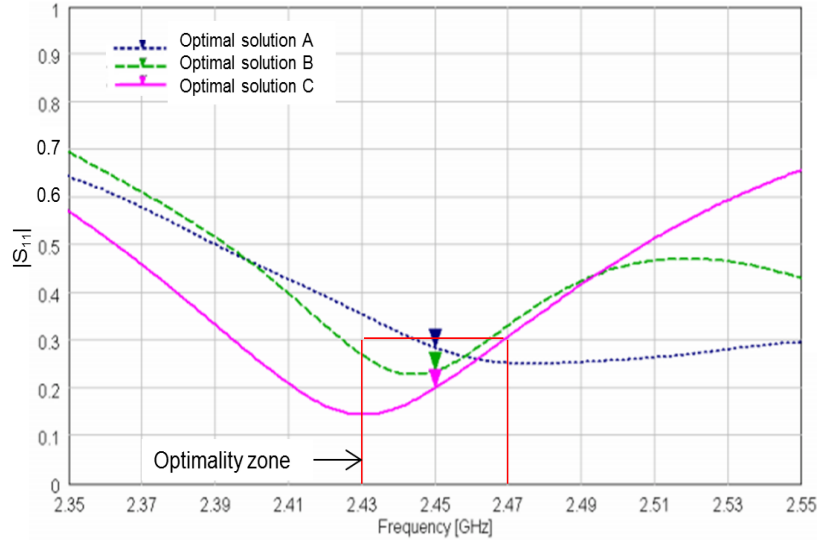
16
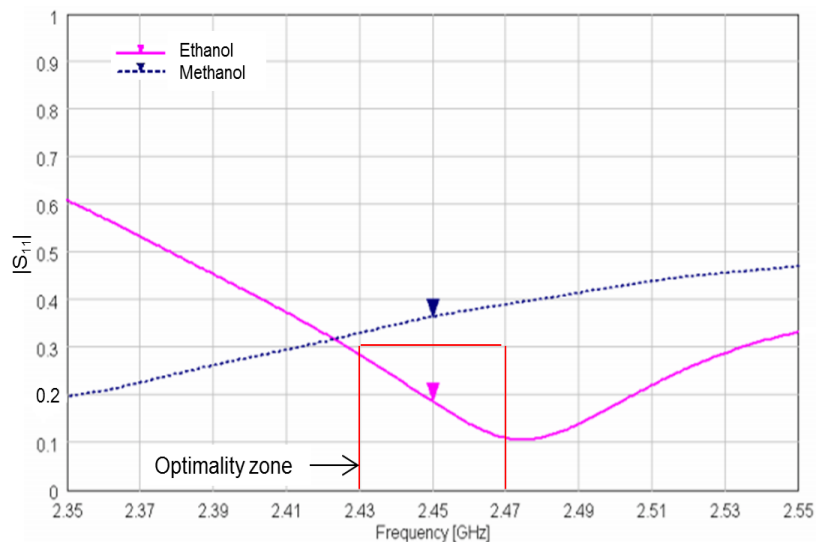
Figure 3.7. Optimization output: best frequency characteristics of the reflection coefficient for water – solution of

problems A, B and C.

Ethanol: Solution B: $T = 58.5$ mm; $C = 110$ mm; $B = 0$ with $W = 100\%$ (DB: 78 pts)

Methanol*: Solution B: $T = 50$ mm; $C = 103.4$ mm; $B = 10$ and $W = 0\%$ (DB: 100 pts)

It is seen from Figure 3.6 that all three configurations of the enlarged reactor guarantee at least 91% energy efficiency – corresponding values of $|S_{11}|$ at 2.45 GHz are less than 0.3. It also turned out that that while in the accepted space of design variables the optimization ends up with an excellent solution for Ethanol; there is no configuration of the enlarged reactor that would provide the same level of energy efficiency for Methanol. The performed optimization, however, provides the best possible characteristic $|S_{11}|(f)$ (and corresponding configuration of the reactor) for this reactant.

3.6 Computational Resources

The *QW-3D* model used in the above optimization represents a hypothetical enlarged analog of *MiniFlow 200SS* batch system and, as such, naturally requires extended computational resources. The upgraded
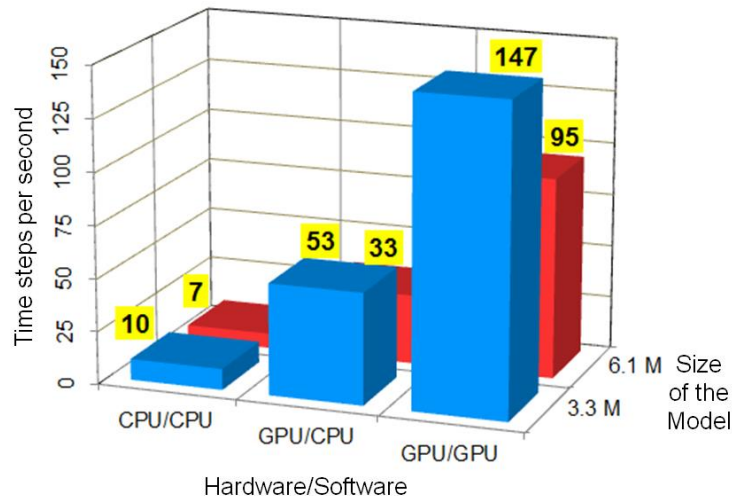
Figure 3.8. FDTD speed in solving the models of 3.3 and 6.1 million cells. CPU Hardware: Workstation A

(CPU only – Table 3.1); GPU Hardware: Workstation B (CPU and GPU – Table X); CPU Software:

QW-OMP simulator; GPU Software: QW-GPU simulator.

Table 3.1. Computational Resources Used in Optimization

Workstation A	Dell T-4700, 64-bit Windows XP, 2 quad-core Intel Xeon 3.20 GHz processors
Workstation B	Microway Xeon+Tesla GPU WhisperStation, 64-bit Window 7, 2 six-core Intel Xeon 2.93 GHz, NVIDIA "Fermi" Tesla C2070 GPU Processor

model for the reactant of 200 ml has cell sizes ranging, depending on the values of the design variables T, C, and B, from 1.8 to 6.1 million cells; therefore, the model may need up to 610 MB of RAM. Initial computational tests of this model were performed on Workstation A (Table 3.1); it turned out that simulation of the upgraded model took place with FDTD speed decreased, compared to the original model, from 7 time steps per second to 3 time steps per second. A single run of this model up to steady state required therefore about 1 h of CPU time of Workstation A. For this reason, this machine was found to be impractical for the use in the procedure of modeling-based scale up of the considered reactor.

Optimization outlined above was performed on Workstation B featuring a GPU processor. To extract maximum productivity from this hardware resource, *QW-GPU*, a GPU version of *QW-3D* FDTD

simulator, was also used. The resulting significant speed-up in computational performance is illustrated in Figure 3.8 for the mid-size model (required 3.3 MB RAM) and the max-size model (required 6.1 MB RAM). In this advanced computational environment, the longest optimizations (which required up to maximum 100 FDTD simulations) took 7.7 hours of CPU time of Workstation B.

4. Conclusions

The results of this MQP confirm excellent suitability of the neural network optimization procedure [12] for determining an enlarged configuration of a batch MAC reactor that possesses desirable energy efficiency. The geometry of the scaled up reactor (considered as an enlarged analog of *MiniFlow 200SS* batch reactor) has been determined as an output of three-parameter optimizations with the objective function associated with the reflection coefficient minimized at a small frequency interval around 2.45 GHz. The capability of the technique to operate with a small number of direct FDTD analyses makes this approach applicable to scenarios with more design variables and of more complex configurations of the reactors.

Earlier, the technique [12] was applied to scale up only a fictional MAC reactor; in this project, we have considered an existing commercially available apparatus. This allowed us to experimentally verify the model prior to optimization, and emphasizes an intrinsic practicality of our approach.

Overall, our results suggest that application of modeling-based optimization procedures may be practical for the expedient design of energy efficient MAC systems.

Appendix

QuickWave-3D UDO Scripts

Main Script

```
comment= "SAIREM MiniFlow 200SS TM Cavity";
bitmap= "TMCavity.bmp";


PAR( "Small Cavity Model A", scavity, "tm" );


# Main cavity cylinder
PAR( "Cavity cylinder height", myh, 46 );
PAR( "Cavity cylinder diameter", myd, 96 );
PAR( "Cavity cylinder diamete Original", mydo, 63 );


# Teflon cylinder
PAR( "Teflon cylinder height", tyh, 46 );
PAR( "Teflon cylinder height zero" ,tyh_zero, 21);
PAR( "Teflon cylinder diameter", tyd, 50.5);
PAR( "Teflon cylinder diameter Original", tydo, 27.5 );
PAR( "Teflon cylinder diameter Original R", tydr, 27.5 );
PAR( "Teflon cylinder diameter zero", tyd_zero, 27.5 );


# Air cylinder cut inside Teflon
```

```
PAR( "Air cylinder height", ayh, 32 );
PAR( "Air cylinder height zero", ayh_zero,21);
PAR( "Air cylinder in Teflon diameter", ayd, 23 );
PAR( "Air cylinder in Teflon diameter zero", ayd_zero, 23 );
PAR( "Lenght of sold teflon", lost, 14 );


# Screw in Teflon cylinder
PAR( "Screw in Teflon height", sith, 12.85);
PAR( "Screw in Teflon diameter", sitd, 5 );



# External horizontal cylinder
PAR( "External horizontal cylinder length", hyh, 4.75 );
PAR( "External horizontal cylinder diameter", hyd, 14 );
PAR( "External horizontal cylinder ajustments to length", hyah, 1 );

# Lower metal vertical cylinder
PAR( "Lower vertical cylinder height", poh, 14 );
PAR( "Lower vertical cylinder diameter", pod, 6.3 );


# Horizontal meal cylinder
PAR( "Horizontal cylinder - length", pah, 5.25 );
PAR( "Horizontal cylinder - diameter", pad, 6.3 );


# Horizontal metal rectangular block
PAR( "Horizontal rectangular block lenght", l, 4.5 );
PAR( "Horizontal rectangular block width", w, 6.3 );
PAR( "Horizontal rectangular block height", h, 4 );


# Rectangular air cut in horizontal block
PAR( "Air block lenght", la, 4.5 );
PAR( "Air block air width", wa, 3.6);
PAR( "Air block air height", ha, 4 );


# Rounding cylinder ending horizontal rectangular block
PAR( "Rounding cylinder height", pch, 4 );
PAR( "Rounding cylinder diameter", pcd, 6.3 );


# Space in vertical cylinder of air
PAR( "Vertical cylinder air height", pcah, 4 );
PAR( "Vertical cylinder air diameter", pcad, 3.6 );
```

```
# Small screw connection
PAR( "Screw connection height", sch, 4 );
PAR( "Screw connection diameter", scd, 3 );


# Upper metal vertical cylinder
PAR( "Part 3 - height", pth, 14.5 );
PAR( "Part 3 - diameter", ptd, 6.3 );


#  Air hole in upper vertical cylinder
PAR( "Part 3 air - height", ptah, 10 );
PAR( "Part 3 air - diameter", ptad, 3.6 );


# External excitation
PAR( "Coax line in x-dir.", coaxx, 10 );
PAR( "Coax line in y-dir.", coaxy, 10 );
PAR( "Coax line in z-dir.", coaxz, 10 );


PAR( "Coax line - external diameter", coaxdd, 14 );
PAR( "Coax line - internal diameter", coaxd, 6.3 );
PAR( "Coax line - length", coaxL, 10 );


# Pyrex vial with reactant
PAR( "Wall thickness", th, 1.5 );


PAR( "Bottom's thickness", thb, 1.2 );


#PAR( "Vial's body: ext. diameter", dv, 46 );
PAR( "Vial's body: height", hv, 31);


PAR( "Vial's throat: ext. diameter", dth, 16 );
PAR( "Vial's throat: height", hth, 5 );


PAR( "Vial's top: ext. diameter", dt, 20 );
PAR( "Vial's top: height", ht, 5 );


PAR( "Walls' material", vmed, Pyrex );


PAR( "Vial's body: ext. diameter Zero", dz, 23 );
PAR( "Vial's body: height Zero", hz, 34);


PAR( "Reactant's material", Rmed, water245 );
```

```
PAR( "Reactant's height", hR, 40 );


# Mesh
PAR( "Small cell size", scell, 0.4 );
PAR( "Large cell size", cell, 1.2 );
PAR( "Cell size in z-dir.", zcell, 0.8 );


#Optization change parameters
PAR( "FIX A", fixa, 14.6 );
PAR("FIX B",fixb , 0);


ENDHEADER;


OPENOBJECT( scavity );


MESHPAR( cell, cell, cell, 1, 2, 1, 2, 1, 2, 1 );


# Main cylinder
CALL( "elements/cyv.udo", chimney1, myd/2, myh, 64, air, E, x, y, z, 10 );


# Teflon cylinder
CALL( "elements/cyv.udo", chimney2, tyd/2, tyh, 64, teflon, E, x, y, z, 10 );
CALL( "elements/cyv.udo", chimney2_zero, tyd_zero/2, tyh_zero, 64, teflon, E, x, y,
      z+tyh, 10 );


# Air cylinder inside the Teflon cylinder
CALL( "elements/cyv.udo", chimney3 , (tyd-4.5)/2, ayh+fixb, 64, air, E, x, y,
      z+lost-fixb, 10 );
CALL( "elements/cyv.udo", chimney3_zero , ayd_zero/2, ayh_zero, 64, air, E, x, y,
      z+lost-fixb+ayh+fixb, 10 );


# Screw in Teflon cylinder
CALL( "elements/cyv.udo", chimney4, sitd/2, sith-fixb, 64, metal, E, x, y, z, 10 );


# Outside horizontal cylinder - coax line
CALL( "basic/lih.udo", chimney5 , hyd, hyh+hyah, air, Y, 2, 90, x, y+myd/2-hyah,
      z+poh+h/2, 11 );


# Lower vertical cylinder
CALL("elements/cyv.udo", chimney6, pod/2, poh, 64, metal, E, x, y+(myd/2-fixa)+pcd/2,
      z, 10 );
```

```
# Two horizontal elements - cylinder and rectangular block
CALL( "basic/lih.udo", chimney7, pad, pah+hyh, metal, Y, 2, 90, x, y+myd/2-pah,
        z+poh+h/2, 11 );


CALL( "elements/cubic.udo", chimney8, w, mydo/2-(mydo/2-fixa)-pah, h, metal, x,
        y+myd/2-fixa+(myd/2-pah-(myd/2-fixa))/2, z+poh, 9 );


# Space in cubic of air
CALL( "elements/cubic.udo", chimney9, wa, la, ha, air, x, y+myd/2-fixa+la/2, z+poh,
        9 );


# Vertical cylinder
CALL( "elements/cyv.udo", chimney10, pcd/2, pch, 64, metal, E, x, y+myd/2-fixa,
        z+poh, 10 );


# Space in vertical cylinder of air
CALL( "elements/cyv.udo", chimney10a, pcad/2, pcah, 64, air, E, x, y+myd/2-fixa,
        z+poh, 10 );
CALL ( "elements/cyv.udo", chimney10b, pcad/2, pcah, 64, air, E, x, y+myd/2-fixa+la,
        z+poh, 10 );


# Combining the elements to make a horiz. rectan. elmenet with a hole

MARK( ELEM, ALL, RESET );
MARKFJ( ELEM, chimney10b, PASSIVE );
MARKFJ( ELEM, chimney9, ACTIVE );
JOIN( GLUE );


MARK( ELEM, chimney10a, RESET);
MARKFJ( ELEM, chimney10b, PASSIVE);
JOIN( GLUE );


# Additional combination of elements (by MO)

MARKFJ( ELEM, chimney8, ACTIVE );
MARKFJ( ELEM, chimney10, PASSIVE );
JOIN( GLUE );
MARKFJ( ELEM, ALL, RESET );


MARKFJ( ELEM, chimney9, ACTIVE );
MARKFJ( ELEM, chimney10a, PASSIVE );
JOIN( GLUE );
```

```
MARKFJ( ELEM, ALL, RESET );


MARKFJ( OBJECT, chimney7, ACTIVE );
MARKFJ( ELEM, chimney1, PASSIVE );
MARKFJ( OBJECT, chimney5, PASSIVE );
JOIN( CUT );
MARKFJ( ELEM, ALL, RESET );


MARKFJ( ELEM, chimney8, ACTIVE );
MARKFJ( ELEM, chimney1, PASSIVE );
JOIN( CUT );
MARKFJ( ELEM, ALL, RESET );


# Small screw connection
CALL( "elements/cyv.udo", chimney12, scd/2, sch, 64, metal, E, x,
      y+(myd/2-fixa)+pcd/2, z+poh, 10 );


# Upper vertical cylinder
CALL( "elements/cyv.udo", chimney13, ptd/2, pth, 64, metal, E, x,
      y+(myd/2-fixa)+pcd/2, z+poh+sch, 10 );


# Air space in the upper vertical cylinder
CALL( "elements/cyv.udo", chimney14, ptad/2, ptah, 64, air, E, x,
      y+(myd/2-fixa)+pcd/2, z+poh+sch+pth-ptah, 10 );


# Coaxial excitation

# External conductor of the coax line
CALL( "basic/lih.udo", chimney15 , hyd, coaxL, air, Y, 2, 90, x,
      y+myd/2+hyh, z+poh+h/2, 11 );


# Internal conductor of the coax line
CALL( "basic/lih.udo", chimney16 , pad, coaxL, metal, Y, 2, 90, x,
      y+myd/2+hyh, z+poh+h/2, 11 );


# Port
CALL( "ports/portoy.udo", coaxinp, coaxdd, coaxdd, DOWN, 1, coaxL-4, inp,
      x-coaxdd/2, y+myd/2+hyh+coaxL, z+poh+h/2-coaxdd/2, 11 );


# Vial with material


# Pyrex vial
```

```
dv = tyd - 4.5;
CALL( "sspvr02L.udo", pvial, th, thb, dv, hv, dth, hth, dt, ht, vmed, dz, hz, x, y,
      z+lost, 16);


# Reactant in Pyrex vial
hR0 = 25460/(tyd*tyd); # WRITEF(hR0);
if (hR0+lost+thb) < 23.15 && (hR0+lost+thb) > 22.85 do hR0 = 7.5; endif;
CALL( "elements/cyv.udo", chimneyreactant, dv/2-th, hR0, 64, Rmed, E, x, y,
      z+lost+thb, 10 );


# Air on the top of reactant
CALL( "elements/cyv.udo", chimneyreactair, dv/2-th, hv-hR0, 64, air, E, x, y,
      z+lost+thb+hR0, 10 );


# Air in the upper part of Pyrex vial
CALL( "elements/cyv.udo", chimneytopair, dz/2-th, hz, 64, air, E, x, y, z+lost+thb+hv,
      10 );


# SPs


# Main cavity
CALL( "elements/specx.udo", spx1, 2, x+myd/2, y, z, 6);


CALL( "elements/specxu.udo", spx21, 2,scell, x-tyd/2, y, z, 7 );
CALL( "elements/specxd.udo", spx22, 2,scell, x+tyd/2, y, z, 7 );
CALL( "elements/specyu.udo", spy23 ,2,scell, x, y-tyd/2, z, 7);
CALL( "elements/specyd.udo", spy24,2,scell, x, y+tyd/2, z, 7 );


# Air cylinder in Teflon cup
CALL( "elements/specxu.udo", spxup, 2, scell, x-ayd/2, y, z, 7 );
CALL( "elements/specxd.udo", spxdown, 2, scell, x+ayd/2, y, z, 7 );
#CALL( "elements/specyu.udo", spyup, 2, scell, x, y-ayd/2, z, 7 );
#CALL( "elements/specyd.udo", spy34_down,scell, 2, x, y+ayd/2, z, 7 );


# Screw in Teflon cup
CALL( "elements/specx.udo", spx41, 2, x-sitd/2, y, z, 6 );
CALL( "elements/specx.udo", spx42, 2, x+sitd/2, y, z, 6 );
CALL( "elements/specy.udo", spy43, 2, x, y-sitd/2, z, 6 );
CALL( "elements/specy.udo", spy44, 2, x, y+sitd/2, z, 6 );


# Excitation - cylindrical and flat horiz. parts
CALL( "elements/specx.udo", spx51, 2, x-pad/2, y, z, 6 );
```

```
CALL( "elements/specx.udo", spx52, 2, x+pad/2, y, z, 6 );


CALL( "elements/specx.udo", spx61, 2, x-ptad/2, y, z, 6 );
CALL( "elements/specx.udo", spx62, 2, x+ptad/2, y, z, 6 );


CALL( "elements/specyd.udo", spydown, 2, scell, x, y+myd/2-pah, z, 7 );
CALL( "elements/specyu.udo", spydown, 2, scell, x, y+myd/2-fixa -pcd/2, z, 7 );


# Excitation - upper vertical cylinder
CALL( "elements/specx.udo", spx81, 2, x-scd/2, y, z, 6 );
CALL( "elements/specx.udo", spx82, 2, x+scd/2, y, z, 6 );


# Small screw connection
CALL( "elements/specy.udo", spx91, 2, x, y+(myd/2-fixa)+pcd/2+scd/2, z, 6);
CALL( "elements/specy.udo", spx92, 2, x,y+(myd/2-fixa)+pcd/2-scd/2, z, 6);


CALL( "elements/specy.udo", spx93, 2, x, y+(myd/2-fixa)+pcd/2+ptad/2, z, 6);
CALL( "elements/specy.udo", spx94, 2, x, y+(myd/2-fixa)+pcd/2-ptad/2, z, 6);


# SPs for  air
CALL("elements/specy.udo", spy101, 2, x, y+(myd/2-fixa)+la+pcad/2, z, 6);
CALL("elements/specy.udo", spy102, 2, x, y+(myd/2-fixa)-pcad/2, z, 6);


# SPs for metal
CALL("elements/specy.udo", spy111, 2, x, y+tyd/2, z, 6);
CALL("elements/specy.udo", spy112, 2, x, y+(myd/2-fixa), z, 6);
#CALL("elements/specy.udo", spy113, 10, x, y+tyd/2+pcd/2+pcad/2, z, 6);


# SP in vertical direction
#CALL( "elements/speczu.udo", spzup, 2, zcell, x, y, z+poh+h/2+coaxdd/2, 7 );
#CALL( "elements/speczd.udo", spzdown, 2, zcell, x, y, z+lost+thb+hR, 7 );


CLOSEOBJ;
```

Supplementary Script

```
comment= "SAIREM's Small Pyrex Vial with a Reactant" ;
bitmap= "sspvrL.bmp" ;
```

```
PAR( "Name", oname, "sspvr02L" );


PAR( "Wall thickness", th, 1.5 );


PAR( "Bottom's thickness", thb, 1 );


PAR( "Vial's body: ext. diameter", d, 46 );
PAR( "Vial's body: height", h, 31);


PAR( "Vial's throat: ext. diameter", dth, 16 );
PAR( "Vial's throat: height", hth, 5 );


PAR( "Vial's top: ext. diameter", dt, 20 );
PAR( "Vial's top: height", ht, 5 );


PAR( "Walls' material", vmed, Pyrex );


#PAR( "Reactant's material", Rmed, water245 );


#PAR( "Reactant's height", hR, 40 );


PAR( "Vial's body: ext. diameter Zero", dz, 23 );
PAR( "Vial's body: height Zero", hz, 34);


ENDHEADER;


OPENOBJECT( oname );


# Vial's bottoms
CALL( "elements/cyv.udo", bottom, d/2, thb, 32, vmed, E, x, y, z, 10 );


# Vial's body
CALL( "elements/cyv.udo", bodyv, d/2, h, 32, vmed, E, x, y, z+thb, 10 );
CALL( "elements/cyv.udo", bodyv, dz/2, hz, 32, vmed, E, x, y, z+thb+h, 10 );


# Vial's throaat
CALL( "elements/cyv.udo", throatv, dth/2, hth, 32, vmed, E, x, y, z+thb+h+hz, 10 );
CALL( "elements/cyv.udo", throata, (dth-2*th)/2, hth, 32, air, E, x, y, z+thb+h+hz,
      10 );


# Vial's top
CALL( "elements/cyv.udo", topv, dt/2, ht, 32, vmed, E, x, y, z+thb+h+hth+hz, 10 );
```

```
CALL( "elements/cyv.udo", topa, (dt-2*th)/2, ht, 32, air, E, x, y, z+thb+h+hth+hz,
      10 );


# SPs

CALL( "elements/specx.udo", spx1, 1, x-d/2, y, z, 6 );
CALL( "elements/specx.udo", spx2, 1, x+d/2, y, z, 6 );
CALL( "elements/specy.udo", spy1, 1, x, y-d/2, z, 6 );
CALL( "elements/specy.udo", spy2, 1, x, y+d/2, z, 6 );


CALL( "elements/specx.udo", spx1, 1, x-(d-2*th)/2, y, z, 6 );
CALL( "elements/specx.udo", spx2, 1, x+(d-2*th)/2, y, z, 6 );
CALL( "elements/specy.udo", spy1, 1, x, y-(d-2*th)/2, z, 6 );
CALL( "elements/specy.udo", spy2, 1, x, y+(d-2*th)/2, z, 6 );


CALL( "elements/specx.udo", spx1, 1, x-dth/2, y, z, 6 );
CALL( "elements/specx.udo", spx2, 1, x+dth/2, y, z, 6 );
CALL( "elements/specy.udo", spy1, 1, x, y-dth/2, z, 6 );
CALL( "elements/specy.udo", spy2, 1, x, y+dth/2, z, 6 );


CALL( "elements/specx.udo", spx1, 1, x-(dth-2*th)/2, y, z, 6 );
CALL( "elements/specx.udo", spx2, 1, x+(dth-2*th)/2, y, z, 6 );
CALL( "elements/specy.udo", spy1, 1, x, y-(dth-2*th)/2, z, 6 );
CALL( "elements/specy.udo", spy2, 1, x, y+(dth-2*th)/2, z, 6 );


CALL( "elements/specx.udo", spx1, 1, x-dt/2, y, z, 6 );
CALL( "elements/specx.udo", spx2, 1, x+dt/2, y, z, 6 );
CALL( "elements/specy.udo", spy1, 1, x, y-dt/2, z, 6 );
CALL( "elements/specy.udo", spy2, 1, x, y+dt/2, z, 6 );


CALL( "elements/specx.udo", spx1, 1, x-(dt-2*th)/2, y, z, 6 );
CALL( "elements/specx.udo", spx2, 1, x+ (dt-2*th)/2, y, z, 6 );
CALL( "elements/specy.udo", spy1, 1, x, y- (dt-2*th)/2, z, 6 );
CALL( "elements/specy.udo", spy2, 1, x, y+ (dt-2*th)/2, z, 6 );


CLOSEOBJ;
```

References

[1] P. Lidstrom, J. Tierney, B. Wathey, and J. Westman, Microwave assisted organic synthesis – a review, *Tetrahedron*, vol. 57, pp. 9225-9283, 2001.

[2] C.O. Kappe and A. Stadler, *Practical Microwave Synthesis for Organic Chemists: Strategies, Instruments, and Protocols*, Wiley-VCH, 2009.

[3] N.E. Leadbeater, Ed., *Microwave Heating as a Tool for Sustainable Chemistry*, CRC Press, 2010.

[4] J.D. Moseley, Microwave heating as a tool for process chemistry, In: *Microwave Heating as a Tool for Sustainable Chemistry*, N.E. Leadbeater, Ed., CRC Press, 2010, pp. 105-147. .

[5] A. Holmes, C. Yang, and V.V. Yakovlev, Temperature modeling for process control in micro-wave-assisted chemistry, In: *IEEE MTT-S Intern. Microwave Symp. Dig*. (Seattle, WA, June 2013) (to be published).

[6] J.M. Kremsner, A. Stadler, and C.O. Kappe, The scale-up of microwave-assisted organic synthesis, *Top Curr Chem*, vol. 266, pp. 233-278, 2006.

[7] J. Moseley, Microwave chemistry – green or not? *Chem. World*, March 2011.

[8] N.E. Leadbeater and J.R. Schmink, Use of a scientific microwave apparatus for rapid optimization of reaction conditions in a monomode function and then substrate screening in a multimode function, *Tetrahedron*, vol. 63, no 29, pp. 6764–6773, 2007.

[9] J. Alcázar, G. Diels, B. Schoentjes, Reproducibility across microwave instruments: first example of genuine parallel scale-up of compounds under microwave irradiation, *QSAR & Comb. Chem.*, vol. 23, no 10, pp. 906-910, 2004.

[10] A. Stadler, B.H. Yousefi, D. Dallinger, P. Walla, E. Van der Eycken, N. Kaval, C.O. Kappe, Scalability of microwave-assisted organic synthesis. From single-mode to multimode parallel batch reactors, *Org. Process Res. Dev*., vol. 7, no 5, pp. 707-716, 2003.

[11] F. Lehmann, A. Pilotti, and K. Luthman, Efficient large scale microwave assisted Mannich reactions using substituted acetophenones, *Mol. Diversity*, vol. 7, no 2-4, pp. 145-52, 2003.

[12] E.K. Murphy and V.V. Yakovlev, CAD technique for microwave chemistry reactors with energy efficiency optimized for different reactants, *ACES J.*, vol. 45, no 12, pp. 1108-1117, 2010.

[13] T.V. Koutchma and V.V. Yakovlev, Computer modeling of microwave heating processes for food preservation, In: M.M. Farid, Ed., *Mathematical Analysis of Food Processing*, CRC Press, 2010, pp. 625-657.

[14] *QuickWave-3D*, QWED Sp. z o.o., ul. Nowowiejska 28, lok. 32, 02-010 Warsaw, Poland, http://www.qwed/com/pl, 1997-2012.

[15] T. Nakamura, R. Nagahata, S. Suemitsu, and K. Takeuchi, *In-situ* measurement of microwave absorption properties at 2.45 GHz for the polycondensation of lactic acid, *Polymer*, vol. 51, pp. 329-333, 2010.

[16] T.R. Bump and W.L. Sibbitt, Aqueous solutions of nitric acid and of sulfuric acid, *Industrial and Engineering Chemistry*, vol. 47, no 8, pp. 1665-1670, 1955.

[17] V.A. Mechenova and V.V. Yakovlev, Efficiency optimization for systems and components in microwave power engineering, *J. Microwave Power & Electromag. Energy*, vol. 39, no. 1, pp. 15-29, 2004.

[18] E.K. Murphy and V.V. Yakovlev, RBF network optimization of complex microwave systems represented by small FDTD modeling data sets, *IEEE Trans. Microwave Theory Tech.*, vol. 54, no. 7, pp. 3069-3083, 2006.

[19] E.K. Murphy and V.V. Yakovlev, Neural network optimization of complex microwave structures with a reduced number of full-wave analyses, *Intern. J. of RF & Microwave Computer-Aided Engng*, vol. 21, no 2, pp. 279-287, 2011.

[20] R.G. Regis and C.A. Shoemaker, Constrained global optimization of expensive black box func-tions using radial basis functions, *J. Global Optim.,* vol. 31, no. 1, pp. 153–171, 2005.